



PHOENICS - Your Gateway to Successful CFD

**P
H
O
E
N
I
C
S

N
E
W
S**

**Editorial
PHOENICS at 30**

Summer 2011

PHOENICS was the first commercial general purpose computational fluid dynamics (CFD) code to appear on the market. It was written under the direction of Professor Brian Spalding who has been at the forefront of computational fluid dynamics for as long as the field has existed.

The code was, and is, marketed through Professor Spalding's Company Concentration, Heat and Momentum (CHAM) Limited which is located in Wimbledon Village, London, England.

PHOENICS, the pioneer of CFD software, is celebrating its 30th year of continued existence in October of this year, something of which we, at CHAM, are very proud.

We would like to hear from those who have been using the code perhaps for the entire 30 years of its existence or for whatever period. Please send us "tales from the world of PHOENICS", preferably with photographs, and we will publish a collection of them in a Special Edition of the PHOENICS Newsletter planned for October this year.

This Newsletter describes an important, perhaps unique, feature of PHOENICS and includes articles from Users and Agents based on work done using the code.

PHOENICS may be the *pioneer* of CFD codes but it is still being updated with its solver containing many capabilities which have yet to be fully exploited.

We, at CHAM, look forward to the next 30 years.



	Item	Page
1	EDITORIAL	1
2	NEWS	
2.1	CHAM News	2
2.2	Branch and Agent News	2
2.3	General News	2
3	PHOENICS APPLICATIONS	3
3.1	Relational Data Input	
4	USER APPLICATIONS	
4.1	Atmospheric Dispersion Modelling with PHOENICS at the Scottish Environment Protection Agency	8
4.2	PHOENICS Modelling of Wave Flow over Artificial Surf Reefs	8
5	AGENT APPLICATIONS	
5.1	A Fast Method for 3D CFD Modelling of a Long River Reach	11
5.2	Dynamics of a Falling Droplet	15
5.3	Humid Air Generator at LNE-Cetiat: Modelling Activity	16

2) News and Events

2.1 CHAM News

2.1.1 Timing Comparisons for Parallel PHOENICS-2010 at May 2011 by Stephen Mortimore, CHAM

CHAM is often asked what speed-up parallel PHOENICS gives over the sequential solver. The answer depends on various factors including size of modelling domain, number of solved variables, how computers are linked and what other software is running (eg firewall, anti-virus).

CHAM recently performed trials using a relatively modest test case set up for a client which was large enough to show parallel speed up. The size of the grid was 260 x 260 x 40 with partial solids treatment turned off and computations made for 100 sweeps. Timings are taken from those shown in the result file for CPU time. Two computers were linked using the company LAN with switch operating at 100 mbps.

Test made on single Quad core PC (Win 7 64bit SP1, Intel Core i7 3.06GHz processor)

Sequential solver: 3955 s
Parallel - 2 processes: 2004 s
Parallel - 4 processes: 1330 s

Test made on two Quad core PCs (Win 7 64bit SP1, Intel Core i7 3.06GHz processor)

Parallel - 4 processes: 1038 s (second run gave 1032 s)
Parallel - 6 processes: 754 s

The tests were made without Anti-virus software installed and with Windows personal firewall and User Access Control (UAC) turned off. The four-processes run across two PCs were subsequently re-run with:

- 1) firewall on using settings recommended in TR110 with no noticeable change in CPU time (1034 s).
- 2) UAC switched back to default level; despite an error message at the start of the run about it not being able to write a registry key, the run does continue and it still has a similar time (1033 s).
- 3) Anti-virus enabled which slowed the run slightly (1046 s). The overhead for enabling the Firewall and Antivirus was slightly over one percent which is acceptable. On a client's blade server configuration, running the same case for 1000 sweeps and with a different anti-virus/firewall combination, the overhead was nearer twenty percent.

It will be noted that the time for running with 4-processes on two machines is quicker than running on a single quad-core computer. This is because running Windows OS on the single computer takes time away from the processes running the solver. When the job is split over two computers each computer has spare core to do what Windows requires.

On the above computations the i7 processors hyper-threading was enabled. Runs for four processes (on a

single PC and a two-PC cluster) were repeated first with hyper-threading switched on and then with it off.

Hyper threading	Single PC, 4 Processes	Two PCs, 4 Processes
On	1321 s	1040 s
Off	1281 s	1039 s

When the cores on the processor are fully occupied, it seems that hyper-threading has a small detrimental impact on computation speeds. But when there were spare processors it did not seem to have an impact.

2.1.2 Graduation Time for Ms Rama devi Pathakota, one of CHAM's new Engineers



Rama with her Course Director Dr Evgeniy Shapiro

Ever since I could remember, I was always curious to understand how machines work, which motivated me to embark on a Bachelor's Degree in Mechanical Engineering.

My interest in fluid dynamics guided to me take up the Masters course in Computational Fluid Dynamics at Cranfield University. I soon realised that the course content suited me very well and I enjoyed learning almost all modules.

During the course I focussed on external aerodynamic problems, more specifically on the optimization of lift augmentation techniques for multi-element aerofoil.

Soon after I graduated, I was very fortunate to find myself in the right place at the right time. I started working as a Consultancy Engineer with CHAM. The last 6 months of my work with CHAM have been most enjoyable and I have been working on HVAC problems such as data centres, clean rooms, operation theatres and dam hydrodynamics.

In the last 24 months with Computational (Colourful) Fluid Dynamics, CFD has made me smile in joy and sometimes go crazy. What a CFD specialist always wants to see is steeply descending convergence plot and when the solution diverges it is an absolute nightmare. The same thing applies to "conservation of life", life has both

good and tough times. During tough times (when the solution diverges), I tell myself “Never give up”.

Thanks to Cranfield University and CHAM. In near future, I hope to see myself as an experienced CFD consultant with expertise in a variety of engineering problems. Long way to go!!!

2.2 Agent News

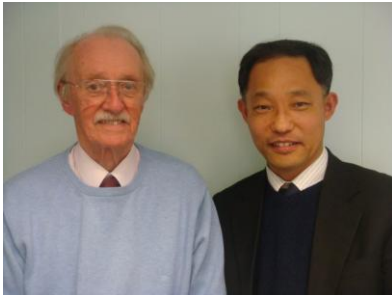
2.2.1 New Agents

CHAM is working with three new Agents to expand PHOENICS sales in their geographic areas:

1) Korea

Innobin Korea Co Pty, Room 702, Frontier Building, 172 Kongnung-dong, Nowon-gu, Seoul 139-743, email: innobin@snut.ac.kr

Professor C-H Kim, pictured below with Professor Spalding on a visit to London earlier this year, has taken over as Agent from Mr Fan of ACT who has relocated.



2) Singapore

ZEB Technology Pte Limited, 213 Kaki Bukit Avenue 1, Shun Li Industrial Park, Singapore 416041 email: andrewkoh@zeb-tech.com, www.zeb-tech.com
ZEB-Technology describes itself as “a visionary green building consultancy firm, which provides expertise to enhance the sustainability for the entire Life-Cycle of both new and existing built environment through a Total Building Performance practice. We strive towards developing a holistic and integrated building design and delivery process to advance green and healthy building design & construction practices. Our organization is committed in rendering services for the creation of a sustainable and healthy environment for the occupants as well as a potential savings in energy through integrated green building strategies.”

3) Turkey

IINORES, Vali Konagi Cad, Haci Mansur Sok, Mim Plaza A Blok No 60, 34363 Nisantasi, Sisli, Istanbul email: serkan.us@inores.com, www.inores.com.

IINORES describes itself as “an engineering company with a vision of providing customer oriented, problem specific and innovative solutions to design and engineering problems. Inores has an analytical and multi-dimensional point of view to engineering problems and has strong relations with University and Research Institutes. Inores brings you the finest Unique, Solution

Specific Engineering products with high skilled and experienced specialists. It has been established by two Aerospace senior engineers with 10+years experience on Computer Aided Engineering.”

The picture below shows, on the left Akgun Kalkan and on the right Serkan Us, the co-founders of Inores. In the centre is Ahmet Fuat Kalcin the CFD engineer who will be responsible for supporting PHOENICS in the area.



2.2.2 PHOENICS in Macau

PHOENICS has moved into Macau and Mr Fan of Shanghai Feiyi held a training course there and provided the pictures shown below.



2.3 General News

2.3.2 CHAM Sponsorship

CHAM is sponsoring Mia, the daughter of one of our colleagues, who with 16 other school friends is taking part in a five week educational expedition to Cambodia and Laos in summer 2012. The trip will

involve a challenging 7 day trek across country and work with local communities, possibly with orphaned children, schools and other similar projects. Mia writes:

“This won't be an average school trip, but a challenging expedition that we hope will benefit the local community as well as teaching us valuable life skills such leadership, communication and team working. We are organising this under the direction of World Challenge which specializes in this type of expedition.

Over the next 14 months our task is to raise £3,595 each to cover our costs. We are organising various events such as discos, odd jobs, supermarket bag-packing, as well as saving all of our birthday, Christmas money and babysitting earnings! One major event for myself and two other friends will be a sponsored walk around the 48 mile Jersey coastline.”



It was that walk which CHAM sponsored Mia to complete in April of this year. We look forward to hearing about the trip to Cambodia in due course.

3) PHOENICS Applications

3.1 What is Relational Data Input?

extracts from a presentation by Brian Spalding, CHAM

It is often necessary to ensure that objects being modelled conform to some rules. Simplistically, if one is modelling a room then a door must fit its aperture, chairs need their legs in contact with the floor and sitters must make contact with their seats.

If one models a particular set-up and wishes to model it using a different room layout, one does not want to have to start over again. Therefore, if the position of the aperture changes, it helps if the door moves with it.

PHOENICS has long had a grouping feature enabling relative-position connections to be expressed and recorded in a Q1 file but not allowing parts of a group to change relative size or position.

This has been remedied and PHOENICS now enables its users to set up classes of scenario which are selected by way of user-chosen parameters. This marks it out from most CFD packages which allow the setting up of single-instance flow-simulation scenarios only. The feature is facilitated via PHOENICS Input Language (PIL) augmented by In-Form.

PIL initially contained assignment statements, IF-statements and declarations, but subsequently had its

capability augmented. This could be described as Advanced PIL which can express relationships between sizes and positions of different objects in a scenario.

Plant placed formulae in a Q1 file which, after satellite interpretation, caused corresponding Fortran coding to be created, compiled and linked to the solver.

In-Form allows users to extend PHOENICS simulation capabilities **without** requiring Fortran coding to be created, compiled or linked into a new executable.

More recently PIL, PLANT and In-Form statements were protected from obliteration by having ‘SAVE’ markers placed before and after them, warning the VR-Editor to save the statements and place them properly in the Q1 file which it was writing. Thus came into existence the ‘protected mode’ of satellite operation.

Relational Data Input: Example 1

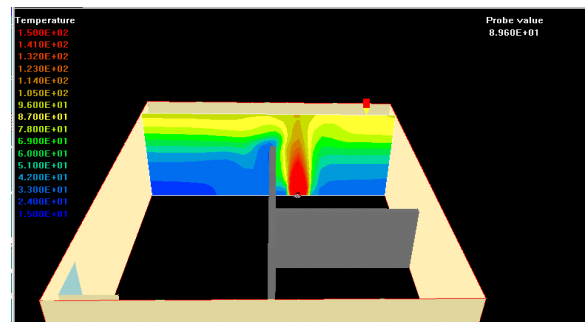


Figure 1

Figure 1 shows instantaneous temperature distributions calculated on the assumption that a fire is burning on the floor of a partitioned room. Use of the protected mode of satellite operation enables relationships to be expressed and preserved in Q1 files so that all features of advanced PIL are available to users of the VR-Editor *via* its in-built text editor.

Differences between old, and new (protected), Q1 files would show that the latter contained additional abilities which save various features. In the diagrams below the logical variable ‘zup’ (z-direction is ‘up’) has been saved.

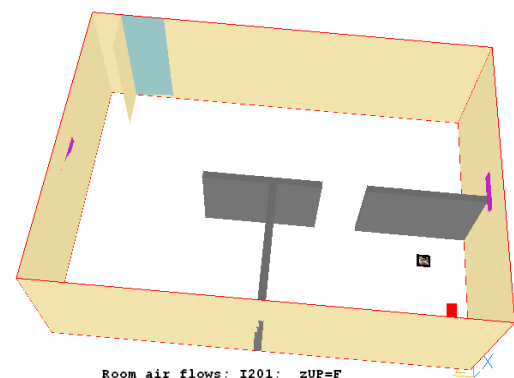


Figure 2

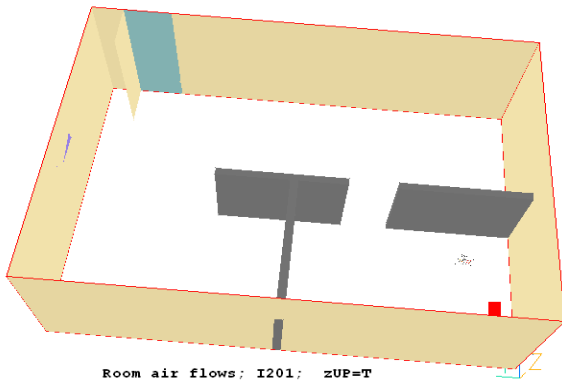


Figure 3

The two diagrams look the same. However, the top one shows zup-f as a default value. When, during the VR-Editor session, the Q1 file is hand-edited and zup = t is set, saving and loading the working files leads to creation of what looks like the same picture but close examination shows the axes are differently lettered. Advanced-PIL lines in the Q1 have made the changes in response to setting a single variable: zup. This would have been very time-consuming to achieve manually.

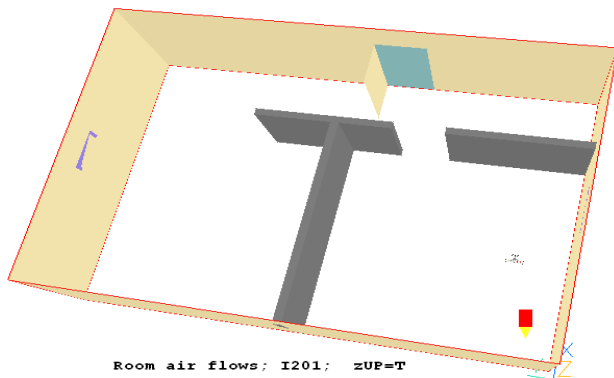


Figure 4

In this figure, of the same room as shown in Figures 2 and 3, the door and partitions have been moved. This was effected by opening the Q1 for editing in VR-Editor mode then finding, and changing, three of the variables contained there, namely:

- Doorzpos: which governs the position of the door;
- Doorhigh: which governs door height
- Prt1wide: which affects the lowest partition width (on the picture).

The wall aperture has changed its position and height in accordance with the door and all partitions have changes size or position to preserve the relationships implied by the Q1.

If it is desired to remove the partitions and/or the fire temporarily from the scene this can be done simply, *via* the built-in editor, during a VR-session as follows:

- a. in imitation of what has been done for 'zup' declaring new Boolean variables 'nopart' and 'nofire';
- b. setting them = t or = f as desired;

- c. on the line above those defining partition-object attributes, inserting the lines:
if(nopart) then
goto nopart
endif
- d. on the line below the attribute-defining lines inserting: label nopart
- e. making the corresponding insertions above and below the fire-object lines

It will then be found that when the Editor is run the partitions and fire are present or absent according to the settings of the respective variables. This is an example of how the protected mode allows useful variables to be declared and used without being obliterated.

Advanced PIL allows interactive modification of settings where PHOENICS can be used to perform the role of a calculator via suggested mathematical operations or where these operations can be edited by hand.

New objects can be introduced interactively. This has been the case for some time but use of Advanced PIL allows relational introduction *via* its do-loop feature. Thus, whereas it has been possible to introduce one man as per Figure 5 it is now possible to introduce more than one as per Figure 6.

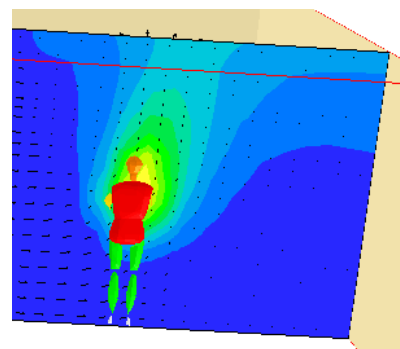


Figure 5

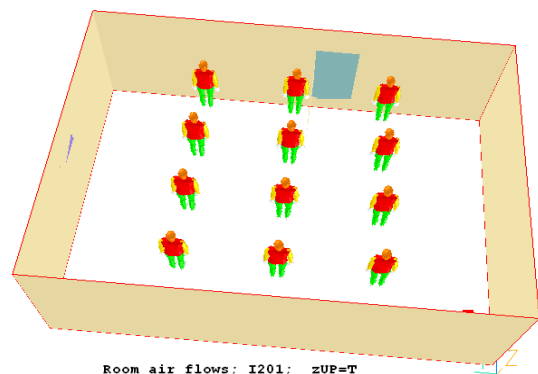


Figure 6

Figure 6 shows results when the VR-Editor is activated. Row and column numbers can be changed by declaring and setting variables 'nmanx' and 'nmany'. Further lines can also be placed in a protected Q1 which varies figure size as in Figure 7

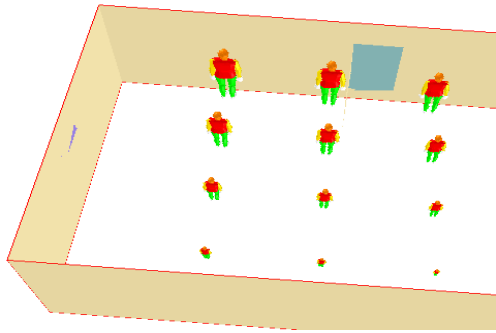


Figure 7

Results are obtained by running the PHOENICS solver and then the VR-viewer. Figure 8 shows warm air rising from the figures as positioned in Figure 6.

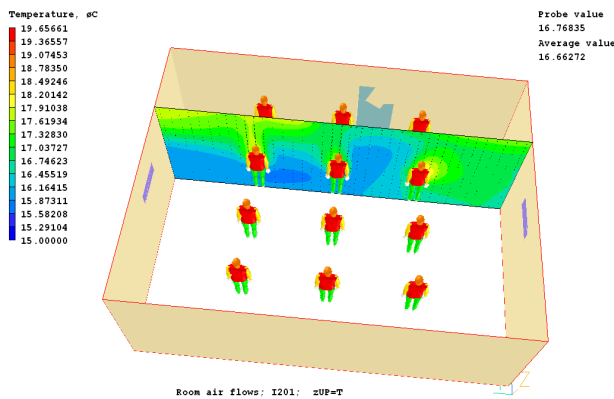


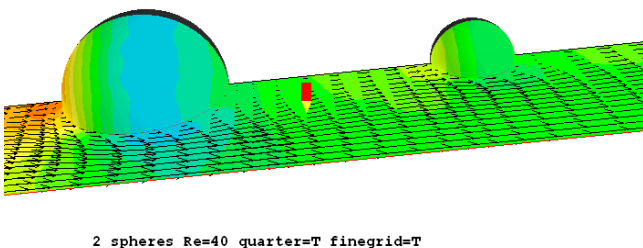
Figure 8

To summarize:

- 1) Protected-mode Q1's are easier to read and edit because they contain more understandable words and fewer numbers;
- 2) If the words used are the names of declared PIL variables they can express relationships between positions and sizes of individual objects;
- 3) More complex relationships can be expressed than have been described here which can also contain non-geometric variables such as sources, initial values, material properties and time.
- 4) Protected mode allows users freedom to choose to work interactively but not to have so to do.
- 5) The ability to enter relational data is an indispensable requirement for a modern CFD code.

Relational Data Input: Example 2

The following hydrodynamic example shows use of Relational Data Input to model flow past objects in a wind tunnel using the protected mode described above.



2 spheres Re=40 quarter=T finegrid=T

Figure 9

Figure 9 shows two spheres one behind the other. This is an existing CHAM Case (number 807) which can be obtained from the CHAM Library and loaded into the VR-Editor when users can change input data as desired. In this particular case provision is made to solve for only one quarter of the domain which is allowed, by reason of symmetry, and is desirable for economy and accuracy. This involves choosing between the two situations shown in Figures 10 and 11 below:

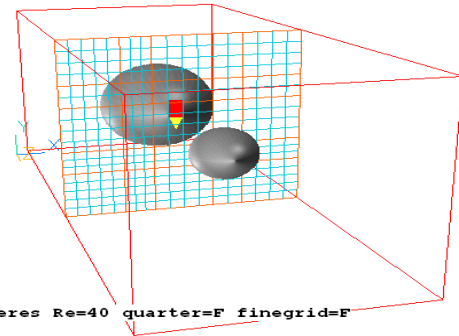


Figure 10

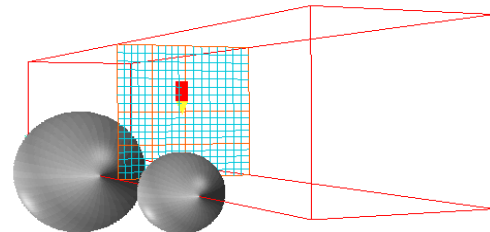


Figure 11

PHOENICS allows more options; but these two are those chosen to exemplify the case here.

In unprotected mode the Editor accepts sizes and positions for each object in a single scenario and records them as numbers which is fine. In protected mode users can create a range of scenarios and record sizes and positions as relationships which is an improvement.

Key and derived parameters must be selected; in this case the key parameters are diam1, diam2 and gap which can be used to study of what influences flow, drag, accuracy, etc.

The initial Q1 writing may take some time but needs undertaking only once after which any number of runs can be generated changing one or more of the parameters.

Compared solutions show the effect of running without a fine grid (figure 12) and then setting 'finegrid=t' (figure 13). The results are qualitatively similar but differences show the necessity of the fine grid:

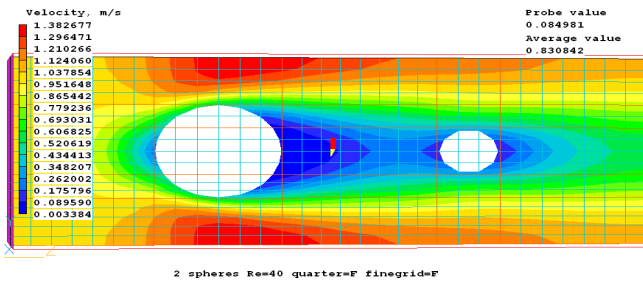


Figure 12

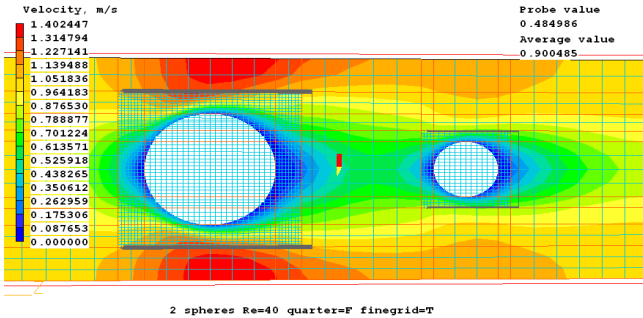


Figure 13

The above figures show comparisons for the full domain. Those below show the same comparisons for the quarter domain where, although the maximum velocities are closer, the contours show at least a display flaw at the base. Figure 14 shows the run without a fine grid and Figure 15 that where finegrid=t:

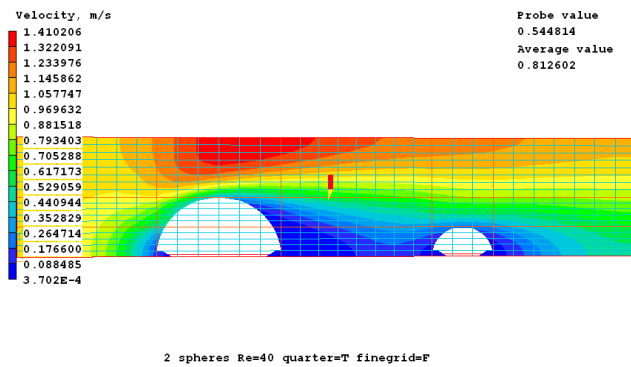


Figure 14

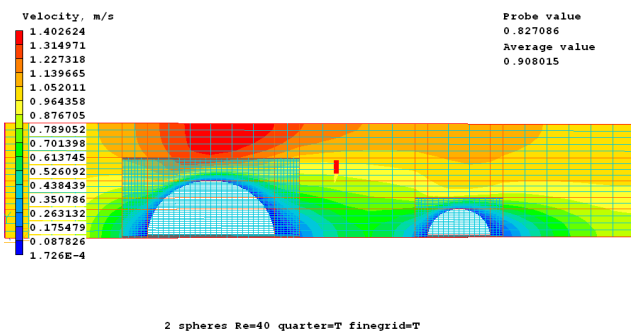


Figure 15

Here it is good to mention a valuable feature of PHOENICS, namely PARSOL, which overcomes tiresome grid-generation problems and is therefore regarded by users as one of the best features of the software.

In these computations the variable PARSOL = t meaning that the mass- and momentum-conservation equations for cut cells at the sphere surface were given special

treatment. Figure 16 below shows the smoothness of pressure cells at the sphere surface which is good despite the grid cells not being extremely small.

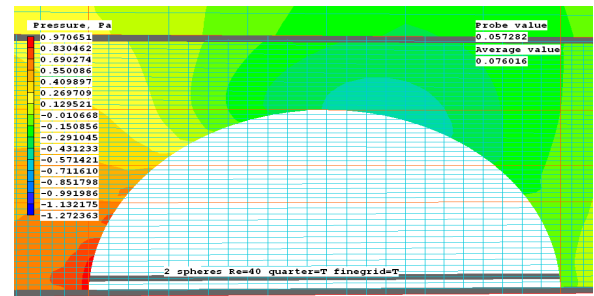


Figure 16

The same is true for any of the computed variables. Figure 17 shows stagnation pressure, Figure 18 y-direction velocity and Figure 19 x-direction velocity. All are as smooth as can reasonably be desired.

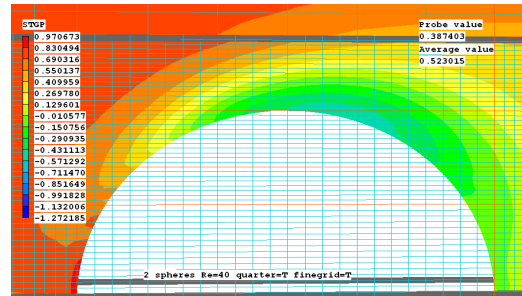


Figure 17

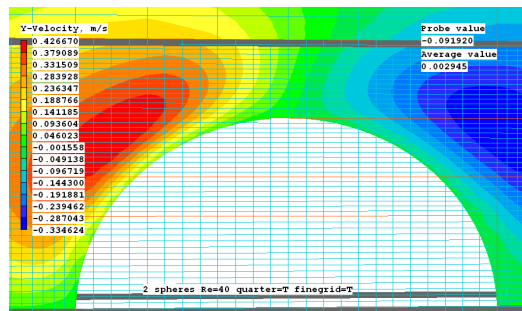


Figure 18

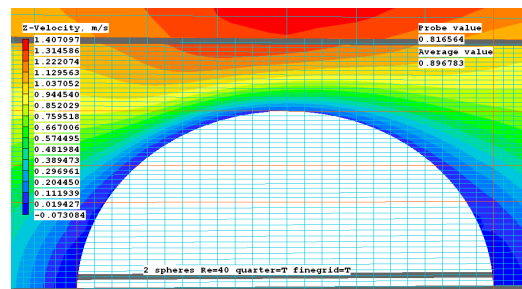


Figure 19

There are other, related, features such as the multi-run capability which can further reduce the input required from users. It is hoped that the contents of this article are sufficient to indicate to readers the value of the RDI feature.

Tutorials are available from CHAM which will assist PHOENICS Users to access those features necessary to use the Relational Data Input feature successfully.

4) User Applications

4.1 Atmospheric Dispersion Modelling with PHOENICS at the Scottish Environment Protection Agency

By Fraser Gemmell, Alan Hills and Alan McDonald

Introduction

SEPA, in conjunction with the support staff at CHAM, have been investigating the use of CFD to model the atmospheric dispersion of pollutants emitted from industrial sites. This is a new approach for SEPA and the work is at an early stage. CFD gives us an additional capability to the widely used Gaussian-type dispersion models; and allows us to better understand the effects of site factors including buildings, stack height, terrain, and meteorological conditions. We can also examine the influence of particular model choices (such as the turbulence model) on the dispersion results.

Results

As an example of some initial results obtained from PHOENICS, Figure 1 shows the increase in ground level tracer concentration with distance downwind from a source, under neutral conditions with a constant wind velocity. Three cases are presented, each having a different combination of stack height and the presence or absence of buildings (Table 1). Comparing Case 1 with Case 3, shows that, under the conditions modelled, the 50 m increase in stack height reduced ground level concentration by an order of magnitude at a distance of 3 km. The difference between Case 1 and Case 2 is relatively small, and the CFD approach suggests that the existing location of the buildings will not adversely impact pollutant levels in this particular case.

Figure 2 shows the Case 1 buildings and stack, and the tracer plume emitted from this source, in the PHOENICS VR viewer.

Case	Stack Height (m)	Buildings
1	155	present
2	155	absent
3	205	present

Table 1. Three different scenarios modelled in PHOENICS.

Conclusion

Initial results suggest that the PHOENICS CFD tool can give us a different modelling perspective at complex sites. This extra information has the potential to aid decision making and help reduce the risk of environmental levels exceeding air quality standards. Thus far, we are able to run PHOENICS with a neutral atmospheric stability. In the future we plan to also incorporate stable and unstable atmospheric boundary layers. In addition the work will be extended to include building and terrain information imported from CAD files; comparing results with other types of dispersion models, and with on-site measurements of air pollution levels. SEPA would welcome contact from other users

of PHOENICS who are involved in similar applications.

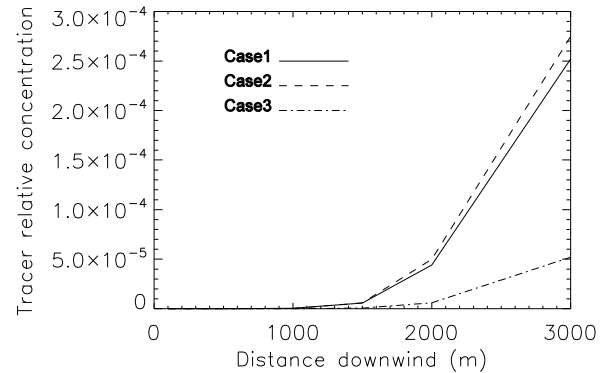


Figure 1. Modelled tracer levels downwind of a source at 2 m height

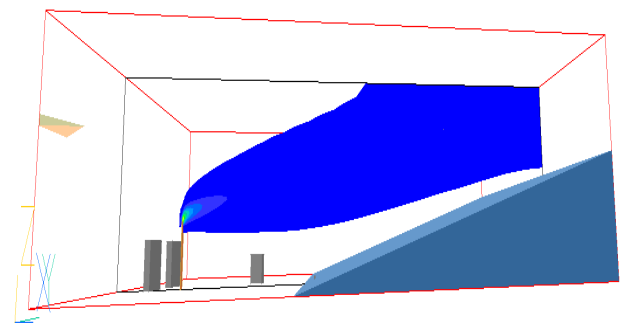


Figure 2. Case 1 in the PHOENICS VR viewer, showing dispersion of a tracer in the atmospheric boundary layer. The 0.001 tracer contour level is shown.

4.2 PHOENICS Modelling of Wave Flow over Artificial Surf Reefs

by Dr R P Hornby

Introduction

Artificial surf reefs are constructed in an attempt to improve the surfing capabilities of coastline, thereby increasing the appeal of the location for surfers and the possibility of increased revenue from shops and cafes servicing the needs of surfers and onlookers. Particular attention has recently focussed on the artificial surf reef constructed at Boscombe, close to Bournemouth on the south coast of England (figure 1).



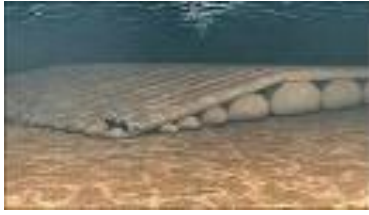


Figure 1 (Top) Aerial view showing Boscombe reef (the underwater shadow) situated about 250m from the shore in water of 3m to 4m depth. (Bottom) Reef construction from sand filled bags.

This is the first such reef to be constructed in Europe. The building of the surf reef at a cost of about £3m has encouraged considerable investment in the local infrastructure and the return on this investment depends to an extent on the performance of the surf reef. However, the reef has not performed as well as expected by surfers and the problems associated with it have been the topic of several recent news items (BBC 1 South Today, 31st March 2011).

As a general guideline, waves break when

$$d = cH \quad (1)$$

where d is the water depth, H the peak to peak wave height, and the constant c is 1.28 (ref 1, although c may vary approximately in the range 1.0 to 2.0 depending on incident wave type). If for simplicity a sinusoidal wave front parallel to the sea bed contours is considered then in the absence of energy loss due to bed friction or turbulence, the wave height as a wave progresses shoreward is given by equation 2 below which can be readily calculated as a function of depth and wavelength (ref 2). C_g is the Group wave speed. The subscript 0 is used to denote initial values.

$$H = H_0 \left(\frac{C_{g0}}{C_g} \right)^2 \quad (2)$$

The shoaling coefficient, K_s , is given by H/H_0 . Figure 2 shows the values of K_s as a function of depth and wavelength. This shows that K_s becomes independent of wavelength for waves with wavelength greater than about 60m. This is a desirable feature of a surf beach since it implies that waves of a given height tend to break at the same point irrespective of wavelength. It is an even more desirable feature of a surf reef since for a given wave height, wave breaking can be fixed on the reef for a range of wavelengths. The Boscombe reef with wave periods of order 7s (40m wavelength) does not quite satisfy this requirement. Tidal effects may also influence a surf reef performance; it is important that the tidal range should be small compared to the depth at which breaking occurs on the reef. If this is not the case then the wave breaking position on the reef will vary with the time of day or may not occur at all. The Boscombe reef is situated in 3m to 4m of water with a tidal range of about 1m, so tidal effects will be important.

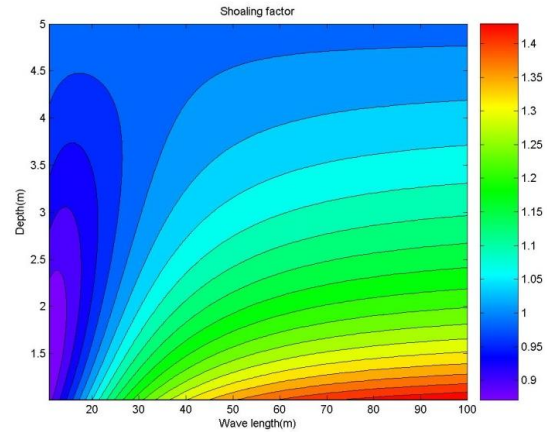


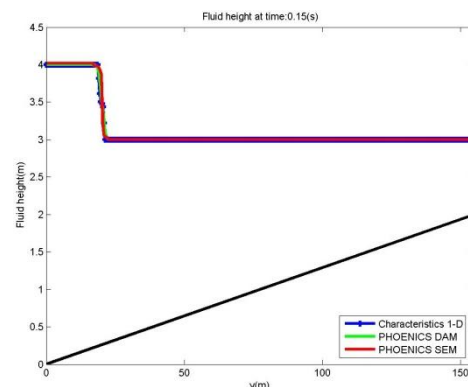
Figure 2 Wave shoaling factor as a function of depth and wavelength.

Simulation modelling

Flow modelling can play a very useful role in understanding the physics of breaking waves on a shelving shoreline and therefore the design characteristics of a surf reef. With this in mind, an investigation has been carried out using PHOENICS to model wave flows over an idealised surf reef, similar in scale to the Boscombe surf reef. Of the possible PHOENICS modelling methods (see POLIS) the Scalar Equation Method (SEM) has been selected. A Depth Averaged Model (DAM) available in PHOENICS by employing the analogy between isentropic compressible flow and the depth averaged Navier Stokes Equations is also used. This offers a simplified, less computationally expensive approach but is only expected to be valid where vertical fluid accelerations are relatively small. In addition, some of the initial testing of the PHOENICS SEM and DAM modelling has been carried out by comparison with the (independent) Method of Characteristics (MOC) (ref 3).

Sea bed friction is calculated using wall functions in SEM and a Chezy formulation in DAM and MOC. Turbulence is not represented in any other aspects of the modelling. The majority of the PHOENICS modelling has been implemented using INFORM which provides an easy way to represent complicated source terms. However, some problems have been encountered - the advice from this work being to represent the source within the INFORM statement using COVAL(Coefficient,Value).

Initial simulation tests



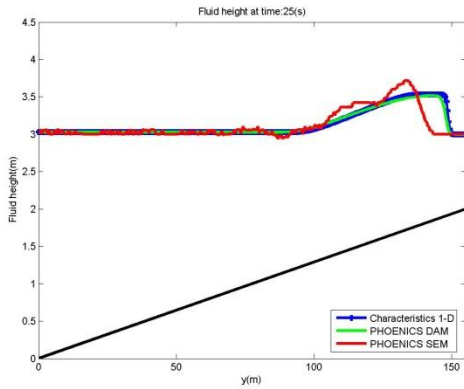


Figure 3 (Top) Initial fluid height above slope. (Bottom) Comparison of fluid heights after 25s.

The depth averaged Navier Stokes equations can be solved very efficiently when there is only one spatial dimension by using the MOC. Comparison results are shown in figure 3 for the slumping of a water column up a slope of length 155m and gradient of 2/155.

The agreement between the PHOENICS DAM and MOC is, as expected, very good for equivalent spatial and temporal discretisations (0.39m in the axial (y) direction with a 0.05s time step). SEM (with the same discretisation in the y direction but about half the time step for stability) gives a more detailed 2-D spatial representation of both the water and air flow above the ambient water level of 3m depth. The results for SEM are, however, similar to those from DAM and MOC, although the wave speed is slightly slower

Grid refinement studies have been carried out for SEM for the above geometry but with an input wave(period approximately 7s) forced by a sinusoidal oscillating source (operating for half a wave period). The results are shown in figure 4 and show little change for the spatial or temporal discretisations shown. These results have then been used in guiding the choice of cell size and time step for the surf reef which has similar dimensions and water depth to the test cases.

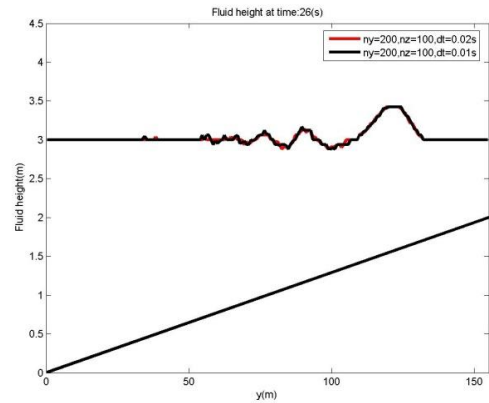
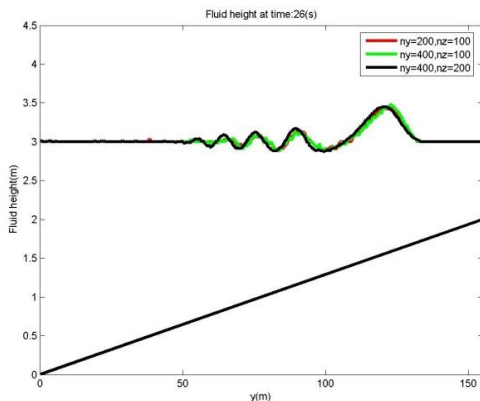


Figure 4. (Top) Comparison of SEM results at 26s (using various spatial discretisations) for given input wave generated by a sinusoidal oscillating source over a half wave period. (Bottom) Comparison of results using two different time steps (200 and 400 timesteps per wave period).

Simulation results for an idealised surf reef

Figure 5 shows an idealised 2-D design for a surf reef with similar dimensions and water depth to the Boscombe surf reef and which is placed on a uniformly shoaling sea bed.

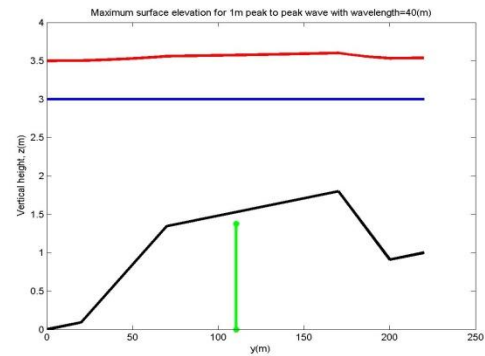


Figure 5. Idealised surf reef geometry showing ambient 3m water depth (blue), maximum predicted water level (equation 2, red) and expected wave breaking point (equation 1, green). Waves move shoreward from left to right.

The surf reef starts with an initial gradient which is large in comparison to the sea bed slope in order to promote rapid steepening of incident waves. This is then followed by a longer less steep section (in this case the gradient is set equal to the sea bed gradient) on which the wave is expected to break relatively early on. The minimum depth for this design is 1.2m. The maximum predicted water height (equation 2) for a 1m peak to peak sinusoidal wave is plotted together with the point at which wave breaking would be expected (equation 1).

Typical surfing waves near the shore at Boscombe have a peak to peak amplitude of about 1m with a near 7s period. This period equates to a sinusoidal wavelength of about 40m. The SEM is used in PHOENICS simulations as this method can predict wave breaking. Waves are generated using a sinusoidal forcing function at the inlet with the appropriate wave period. The domain shown in figure 5 is discretised with 400 cells in the y direction

(along the reef) and 100 cells in the vertical direction. Each wave period is divided into 200 time steps.

Figure 6 shows results and also illustrates effects of grid sensitivity by variation of spatial and temporal step sizes in relation to the above mentioned grid.

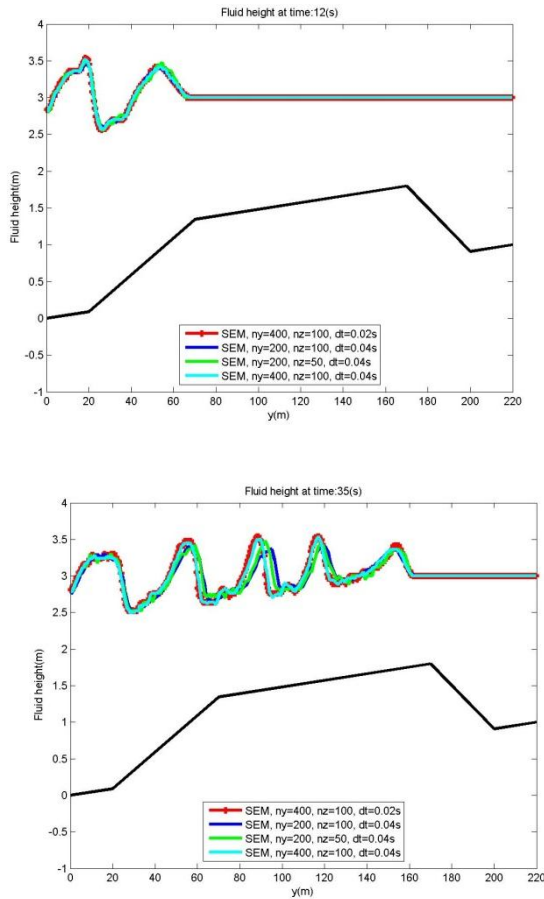


Figure 6. Wave propagation over the surf reef using different spatial and temporal discretisations. (Top) After 12s. (Bottom) After 35s.

There is seen to be little change in results from changes in grid discretisations. Results show a steepening of the waves as they propagate over the surf reef, a reduction in wave speed and a small initial increase in wave height, but no evidence of wave breaking.

The wave pattern over the reef is still developing. It is not clear from what has been done so far as to whether a cyclical wave pattern is formed – a larger number of input wave periods needs to be represented - with wave breaking forming part of the cycle.

Conclusions

The PHOENICS Scalar Equation Method has been used to model the 2-D wave flow over an idealised surf reef in water depths and with spatial scales similar to those of the Boscombe surf reef. Initial results illustrate the expected wave steepening and phase speed reduction over the reef, but the expected wave breaking has not, so far, been captured in the simulations. This may be due to the requirement for a much finer spatial grid (the

coarser grid effectively smoothing out a breaking event) or a longer transient to enable development of a cyclical wave pattern. These aspects will be investigated in future work as well as comparisons with physical model data.

References

1. Chadwick A, Morfett J. Hydraulics in Civil engineering. Allen and Unwin 1986.
2. Lighthill J. Waves in Fluids. Cambridge University Press 1979.
3. Whitham G B. Linear and Nonlinear Waves. John Wiley and Sons Inc.1999.

Dr R. P. Hornby e-mail: bob@hornby007.wanadoo.co.uk

5) Agent Supplied Applications

5.1 ACFDA

A FAST METHOD FOR 3D CFD MODELING OF A LONG RIVER REACH

by S. Kwan¹, J. A. Vasquez², R. G. Millar³, P. M Steffler⁴

ABSTRACT

An innovative method for modelling the three dimensional flow in a long river reach is presented. The technique involves coupling River2D, a two dimensional depth averaged hydrodynamic model with a three dimensional CFD model. The depth averaged flow of a river is first solved using River2D. Then, using the finite element grid, 3D stereolithographic files (STL) of the river bed and the water surface elevation (WSE) are created using a modified version of River2D and imported into PHOENICS, a general purpose CFD package.

The bed file is used as the lower boundary condition and the WSE file is used as the frictionless “rigid lid”. Converged results can be obtained in much less time relative to a 3D free-surface simulation. Results show regions of secondary flow needed for accurately predicting areas of general scour or sediment deposition and areas which are susceptible to local scour.

INTRODUCTION

Flow in large rivers is typically characterized by low water surface gradients and water depths that are relatively small when compared with other horizontal dimensions. Under these conditions, the vertical velocity component is usually not very important when computing the general flow patterns and it can be neglected, as done by two-dimensional (2D) depth-averaged flow models.

However, in certain cases, such as secondary currents in sharp bends, flow around bridge structures (piers and abutments) or spur dykes, the vertical velocity component may be relevant and a three-dimensional (3D) model is required. Typical 3D river flow model such as SSIIM (Olsen 2010), CH3D (Gessler et al 1999) and FAST3D (Wu et al 2000) use structured boundary-fitted

(SBF) meshes to represent the river planform geometry; while several stacked-up horizontal layers are used to take into account the vertical dimension. These simple but efficient meshes allow simulating large domains within reasonable computational time. However, SBF meshes cannot accommodate complex geometries, as those sometimes found when modelling hydraulic structures, which are usually modelled using Computational Fluid Dynamics (CFD) models.

CFD models are general-purpose flow models intended usually for modelling the local 3D details of flow features around geometrically complex solids. In hydraulic engineering, they have been applied for modelling spillways, dams, bridge piers and similar, which cannot be easily modelled using SBF meshes. The solid geometry in CFD models (e.g. Flow-3D, PHOENICS, STAR-CCM+ and CFX) is commonly represented using a stereo lithography file (STL).

An STL file describes a raw unstructured triangulated surface by the unit normal and vertices (ordered by the right-hand rule) of the triangles using a three-dimensional Cartesian coordinate system. The advantage of the STL format is that any conceivable 3D geometry, regardless of its complexity, can be represented and imported into the CFD software.

Specialized drafting software, such as AutoCAD's Civil3D, can be used to transform a river's bathymetric survey into a STL solid for CFD simulation; but this process is usually time consuming and tends to work well only when the point data is regularly spaced (gridded). Few CFD packages, such as Flow-3D, can read directly scatter topographic point data in order to generate a 3D solid; but again this approach works well with uniformly spaced point data. These apparent limitations stem from the fact that CFD models are general and not necessarily intended for modelling rivers with natural bed topography and as such, they lack the basic topographic interpolation routines which are standard in most 2D and 3D hydraulic river flow models.

Three dimensional CFD river models are typically divided into two types: free surface and rigid lid models. Free surface, CFD models normally use the Volume-of-Fluid (VOF) method. This is a sophisticated method that can accurately track the location of the free surface, even in cases with sharp and highly unsteady water surfaces, as those caused by sudden-dam breaks (Vasquez and Roncal 2009). However, the high computational demand of the VOF method is usually not warranted for modelling large river reaches given their relatively small water surface slope.

For this reason, a rigid lid approximation is used commonly instead, in which the water surface is represented as a fixed and frictionless lid, allowing much faster computations. One drawback with this approach is that the geometry of the rigid lid must be known in advanced and input by the user. One way to do this is to use a simpler, more computationally-efficient model to

calculate the water surface elevations that form the rigid lid. For example, SSIIM (Olsen 2010) computes the rigid lid using one-dimensional backwater computations before the onset of the 3D flow computations. However, the disadvantage of this method is that the velocity of the flow may be under or over-estimated in regions where the river meanders if no adjustments to the lid are made. In this paper, we propose a technique that accounts for differences in water surface in bends by using River2D, a two dimensional depth-averaged flow model to compute the rigid lid and also to generate the 3D STL representation of the riverbed.

River2D (Steffler and Blackburn 2002) comprises a suite of specialized programs for modelling flow in rivers. It is possible to generate a topographic surface model from scatter topographic data points, by means of a triangular irregular network (TIN), which can be later interpolated into unstructured Finite Element (FE) meshes made of triangular elements. After computing an initial flow field, the mesh can be further refined based on the computed flow variables (e.g. velocity, depth, etc.), in such a way that the final mesh geometry can reflect not only the river geometry but also the overlaying flow field.

The River2D code was modified to transform this final FE triangular mesh into STL files for both the riverbed and the water surface, which can be then imported into CFD models to perform 3D rigid-lid simulations. This approach has the advantages that the STL solid geometry can be generated almost instantaneously following a triangular mesh that better represents the river geometry and computed flow field.

Additionally, the 2D computed rigid lid takes into account important effects such as flow curvature and the presence of structures (bridges, spur dykes, etc.) and hence it is more accurate than a flat or 1D-computed rigid lid. We selected the CFD model PHOENICS for the preliminary proof of concept reported here; but this method should be applicable to any CFD model that reads STL files (e.g. Flow-3D, CFX or STAR-CCM+).

STUDY SITES

For this preliminary study, we investigated 2 river reaches: the Fraser River situated upstream of the Pattullo Bridge in Vancouver, Canada and the Paraguay River located along the boundary between Bolivia and Brazil. For the Fraser River study site there are extensive velocity measurements collected with an ADCP at a discharge of 7800 m³/s, which is close to mean annual flood (Figure 1). The Paraguay River was simulated to illustrate the 3D flow field around a sharp 110 degree bend. However, no ADCP data was available for this river.

THE PHOENICS MODELS

The CFD modelling was based on version 3.6 of the PHOENICS code which solves the full 3-D Navier-Stokes equations discretized over a finite-volume grid. The pressure and momentum equations are coupled through

the SIMPLEST algorithm (Patankar and Spalding, 1972). To simulate the effects of wall roughness, the roughness height is set at $k = 0.4$ m (same as the River2D bed roughness) for the logarithmic law of the wall turbulent boundary condition. The rigid lid created using the water surface elevation is given a frictionless surface; while the standard $k-\epsilon$ model was used for modelling turbulence.

A free-gridding approach was used which enabled the grid to be changed independently of the geometry. This method, known as PARSOL (PARTial SOLids), performs accurate simulations for complex geometries and can save significant time in setting up a simulation (PARSOL is somehow similar to the FAVOR method used by Flow-3D).

For the Fraser River, the solution domain covers a reach length of approximately 6.5 km. Using a coarse mesh with a uniform cell size of $30 \times 30 \times 1$ a converged solution can be obtained in under 10 minutes. However, a finer mesh was needed to validate the model and capture the fine details around the bridge piers.

For this simulation the domain had $362 \times 269 \times 26$ cells, with the cell size ranging from $60 \times 60 \times 1$ m in the upstream section of the river to $3 \times 3 \times 1$ m in the region around the bridge piers (see Figure 1).

For the Paraguay River, the solution domain covers about 4 km of the river and uses $190 \times 210 \times 32$ cells, with a uniform size of $10 \times 10 \times 1$ m.

RESULTS

Figure 1 shows the flow field computed by the CFD model. In addition to the bed topography and water surface imported as STL files from River2D, the model also included 3D solids representing the piers of 3 bridges plus a guiding dyke that splits flow around an island. This illustrates how simple is to add hydraulic structures to the model.

The computed 3D flow patterns are evident in Figure 2, which shows the velocity field on a vertical plane cutting through the right arm of the Fraser River. The triangles of the solid STL model representing the bed topography in Figure 2 come from the initial River2D mesh.

Figure 3 shows a comparison between ADCP data and computed velocity at two transects located upstream from the Pattullo Bridge. There is reasonable agreement between measured and computed velocity profiles.

The sharp bend in the Paraguay River leads to more complex 3D flow patterns, with eddies on both the horizontal and vertical planes (Figure 4). This is a good example where 3D models can offer useful information on secondary circulation that cannot be obtained by 2D models.

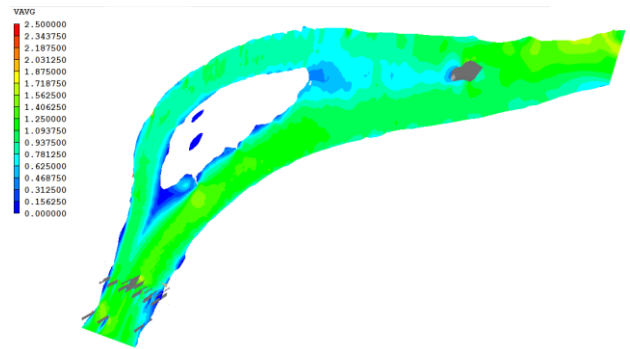


Figure 1. CFD model of the Fraser River showing solid piers in the downstream part and a guiding dyke upstream, plus the computed flow velocity.

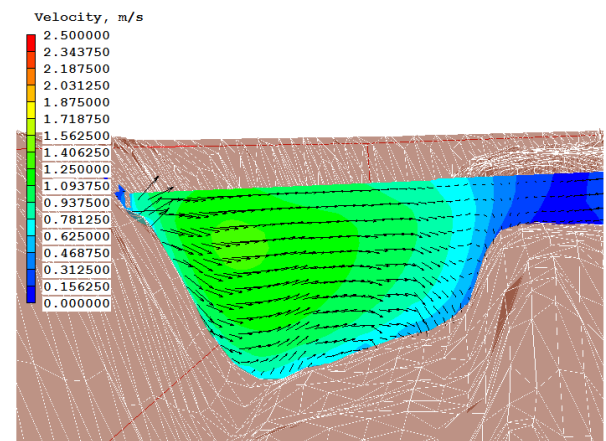
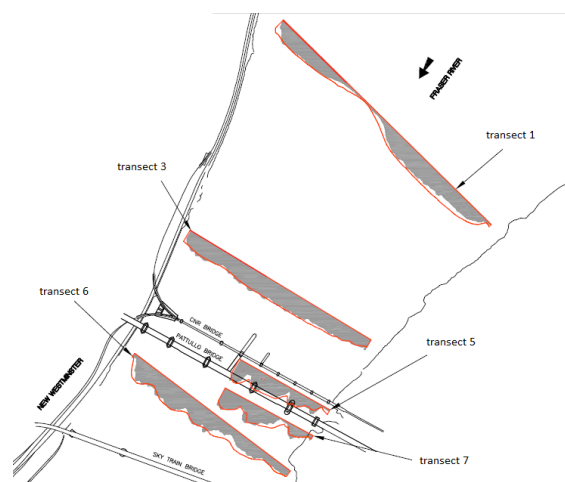


Figure 2. Secondary flow at a transect 1. Contours show streamwise velocity and vectors show lateral and vertical components (triangulated 3D bed surface is the initial River2D mesh transformed into a STL file).



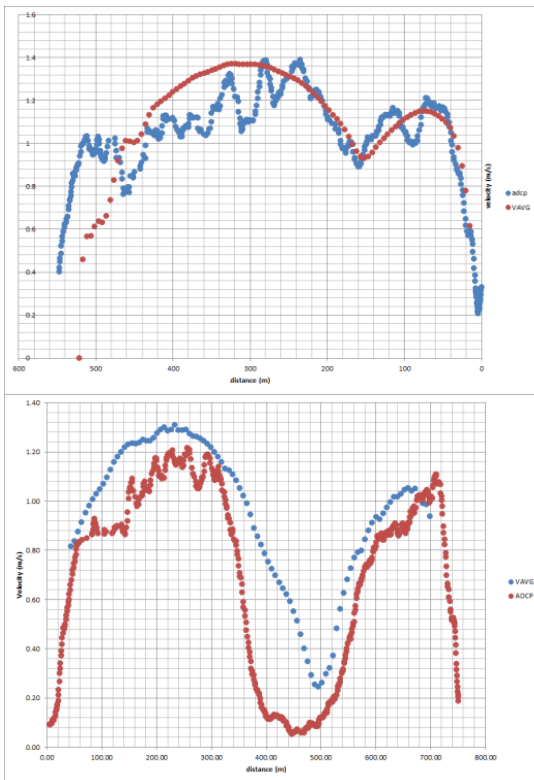


Figure 3. Location of ADCP transects and comparison between computed velocity and ADCP data at transect 1 and 3.

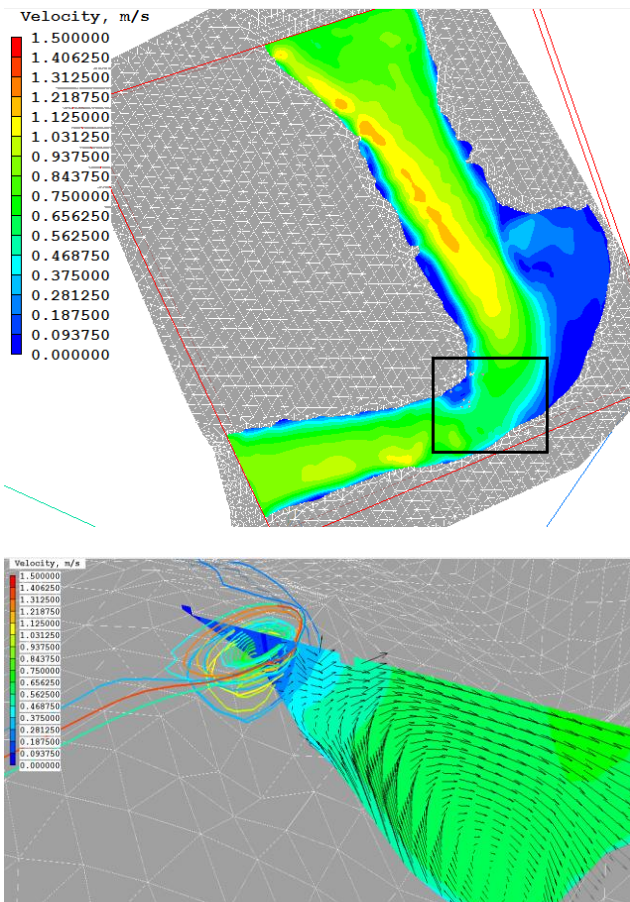


Figure 4. Surface velocity in the Paraguay River (top) and cross sectional view showing the in-plane velocity vectors and circulation region downstream of the bend in the Paraguay River (in boxed area).

CONCLUSIONS

The preliminary tests reported here have demonstrated that 3D rigid-lid CFD modelling of large rivers, performed by computer codes that use STL geometry files, can benefit from using a 2D depth-averaged model to generate the solid models for the bed topography and water surface. The advantages of this approach are that: (1) the 2D flow field can be used to guide the development of the 3D solids, for example, increasing the resolution in areas of higher velocity; (2) the rigid-lid is not flat, but instead incorporates the water surface computed by the 2D model; (3) the computational speed of the 3D rigid-lid model for a large river can be an order of magnitude or so higher than a free surface 3D model.

REFERENCES

- Ferguson R. I., Parsons D. R., Lane S. N., Hardy R. J. (2003). Flow in meander bends with recirculation at the inner bank. *Water Resources Research*, 39(11): 1322-1334.
- Gessler D., Hall B., Spasojevic M., Forrest H., Pourtaher H., Raphelt N. (1999). Application of 3D Mobile Bed, Hydrodynamic Model. *Journal of Hydraulic Engineering*, 125(7): 737-749
- Olsen N. R. B (2010). A three dimensional numerical model for simulation of sediment movements in water intakes with multiblock option, User's manual, 2010. Available at <http://folk.ntnu.no/nilsol/ssiim/manual3.pdf>
- Patankar, S. V. and D. B. Spalding (1972). A calculation procedure for heat, mass and momentum transport in three dimensional parabolic flows, *Int J. Heat Mass Transfer*, 15: 1787-1806.
- Steffler, P. M., and Blackburn, J. (2002). "River2D: Two dimensional depth-averaged model of river hydrodynamics and fish habitat. Introduction to depth-averaged modelling and user's manual." University of Alberta, Edmonton.
- Vasquez, J. A., and Roncal, J.J. (2009). Testing River-2D and Flow-3D for Sudden Dam-Break Simulations. Canadian Dam Association Conference, Whistler, Canada.
- Wu, W., Rodi, W., and Wenka, T. (2000). "3-D numerical modeling of water flow and sediment transport in open channels", *Journal of Hydraulic Engineering*., ASCE, 126(1): 4-15.

¹ MWH Canada, 505 Burrard St, Vancouver, BC, Canada, V7X 1M6; email: Stephen.Kwan@mwhglobal.com;

² Northwest Hydraulic Consultants, 30 Gostick Place, North Vancouver, BC, Canada, V7M 3G3; email: JVasquez@nhc-van.com;

³ University of British Columbia, 6250 Applied Science Lane, Vancouver, BC, Canada, V6T 1Z4; email: Millar@civil.ubc.ca;

⁴ University of Alberta, Water Resources Engineering, Edmonton, AB, Canada, T6G 2W2; email: Peter.Steffler@ualberta.ca

5.2 Arcofluid

Two submissions by Jalil Ouzzani of Arcofluid are contained on pages 15 and 16 below.

Dynamics of a falling droplet

A. LEKHLIFI^(a), M. ANTONI^(a), J. OUAZZANI^(b)

^(a)Aix-Marseille Université – Institut des Sciences Moléculaires de Marseille iSm2 CNRS UMR 6263
Équipe AD2EM – Centre Saint Jérôme – service 451/461 – 13397 Marseille Cedex 20 – France

^(b)ARCOFLUID Parc Innoïvis- 3 rue du Golf - 33700 – Mérignac
adl.lekhlifi@etu.univ-cezanne.fr, m.antonio@univ-cezanne.fr, general@arcofluid.fr
website: www.ism2.univ-cezanne.fr, www.arcofluid.fr

Abstract

The objective of this work is to study numerically the hydrodynamics of a droplet of pure water falling in a continuous oily phase. The model under focus is two-dimensional and includes gravity and the basic physical properties that occur at interfaces like surface tension. Particular emphasis is put on the tracking of liquid-liquid interfaces and on the limitation of numerical diffusion. This is indeed fundamental for a precise description of the phenomena that arise at interfaces in particular between drops in dispersed systems like emulsions. The Phoenix CFD software from CHAM has been used to solve for the described problem.

We assume the two fluids under consideration to be Newtonian and incompressible, with uniform surface tension and no phase change. The evolution of the two-phase flow is described using the one-fluid VOF (Volume of Fluid) formulation of the Navier–Stokes equations solved by the Phoenix code.

The numerical simulations rely on a color function that describes the relative volume fraction of the two fluids. This function is set to one (resp. zero) in cells filled with fluid 1 (resp. 2) and takes intermediate values in the cells belonging to the interface region (fig 1.).

Mathematical model

$$\nabla \cdot \mathbf{V} = 0$$

$$\rho \frac{\partial \mathbf{V}}{\partial t} + \rho \mathbf{V} \cdot \nabla \mathbf{V} = -\nabla P + \rho \mathbf{g} + \mu \Delta \mathbf{V} + \alpha \sigma \kappa \mathbf{n} \cdot \nabla \mathbf{C}$$

$$\frac{\partial C}{\partial t} + \mathbf{V} \cdot \nabla C = 0$$

$$\rho(\mathbf{x}, \mathbf{y}, t) = \rho_{PO} + (\rho_W - \rho_{PO}) \times H(C(\mathbf{x}, \mathbf{y}, t))$$

$$\mu(\mathbf{x}, \mathbf{y}, t) = \mu_{PO} + (\mu_W - \mu_{PO}) \times H(C(\mathbf{x}, \mathbf{y}, t))$$

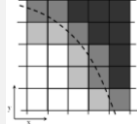


Fig 1 : Schematic plot of the color function in the vicinity of the interface. VOF cells appear as squares and the interface location as a dashed curve. White cells are inside the droplet (C(x,y)=1) and blacks in the paraffin oil (C(x,y)=0). Grey cells correspond to intermediate interfacial region.

Model CSF Continuum surface

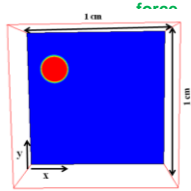


Fig 2 : Example of color function C(x,y,t) for a 200x200 mesh grid at time t=0.2 s. Orientation of gravity field is top down and droplet radius r=1 mm. Water/paraffin oil interface shows a good spatial resolution. Initially the center of the droplet is located at and velocity are all set to zero.

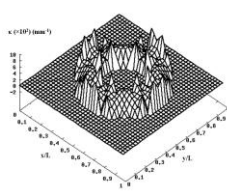


Fig 3 : 3D illustration of the curvature for a droplet radius r=15 mm and for a 40 x 40 Cartesian mesh grid and a box size of 60 mm x 60 mm. The center of the droplet is at x/L=0.5 and y/L=0.5 where L=60 mm is the length of the side of the box.

$$\kappa = 2 \sigma \frac{1}{|n|} \left[\left(\frac{n}{|n|} \cdot \nabla \right) |n| - (\nabla \cdot n) \right]$$

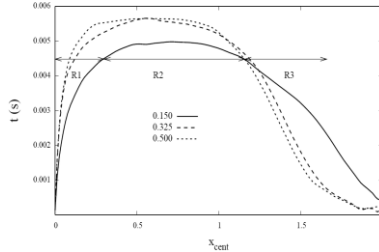


Fig 1 : Time evolution of the average velocity for a r=1 mm droplet at T=298 K. Initial height and positions vary and are given in the legend.

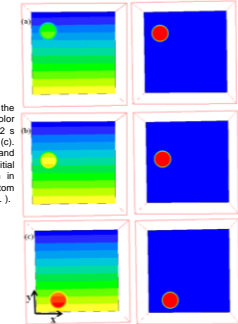


Fig 1 : Contour plot of the pressure field (left) and color function (right) of the interface at time t=0.02 s for three different values of droplet radius: (a) r=1.00 mm, (b) r=1.5 mm, (c) r=2.00 mm. Pressure at the bottom (resp. top) of the box is (resp.) shown.

$$\frac{\partial \phi}{\partial t} + \nabla_s (\phi U_s) = D_s \nabla_s^2 \phi$$

$$\frac{\partial \phi}{\partial t} = \nabla \cdot \mathbf{n} (\mathbf{n} \cdot \nabla)$$

$$\mathbf{g} = 0$$

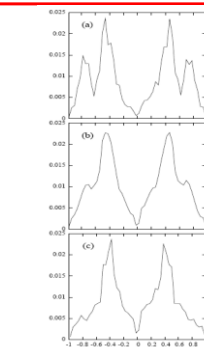
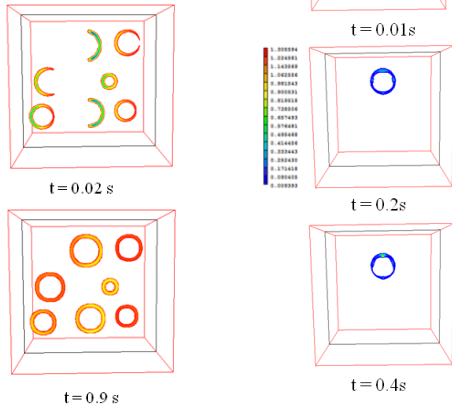


Fig 1 : Averaged interfacial velocity field in the frame of the droplet averaged for different values of droplet radius and mesh grid size. Reference size for velocity arrows is shown in the upper right corner of (c).

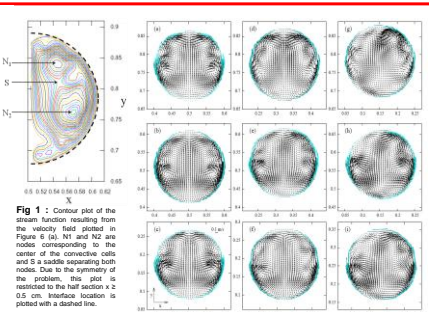


Fig 1 : Velocity field in the frame of the droplet at time t=0.1 s (top line), t=0.6 s (middle line) and t=1.3 s (bottom line) for three different values of droplet radius. Reference size for velocity arrows is shown in the upper right corner of (c).

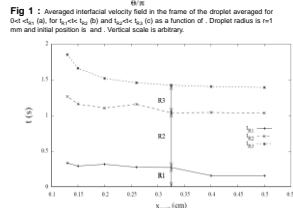


Fig 1 : Values of (v), (t) and (f) as a function of the initial height. The initial height is the same than in Figure 3. Time duration of angle times R1 (), R2 () and R3 () in the case are represented by arrows.

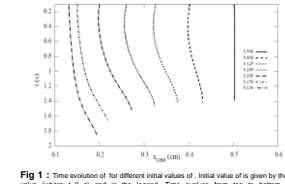


Fig 1 : Time evolution for different initial values of initial value of given by the top value (where h=0) and in the legend. Time evolves from top to bottom. The representation of the trajectories is interrupted at time. The initial height is the same than in Figure 3 for all the simulations.

Conclusions

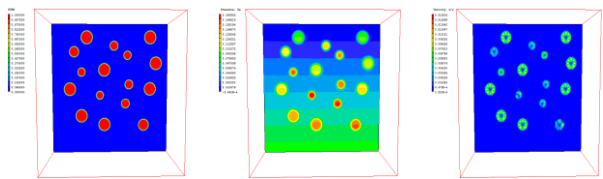
This work presents the method and the results of the simulation of the hydrodynamics inside and on the interface of a water droplet in paraffin oil and under gravity conditions. Good resolution of the interface is achieved and precise predictions are obtained for the velocity distributions and Laplace pressure differences. We have been able to introduce the Brackbill model as well as the surfactant approach in the Phoenix code through Fortran routines.

Perspectives

Role of surface active molecules and interfacial rheology in the dynamics of droplets. Influence of oil soluble surfactants on the time evolution of the droplets.

Brackbill & J.Zemach. *Comput. Phys.* 1993
G.Balmigere, S.Vincent & J.Caltagirone. *Comput. Phys.* 2007
A.Lekhlifi, M.Antoni & J.Ouazzani. *Physico chemical and engineering aspects*, 365, 2010

Simulation of the aging Dynamics of diluted emulsions.



Humid air generator at LNE-CETIAT: modeling activity

Eric Georin ¹, Jalil Ouazzani ²,
¹LNE-CETIAT, Villeurbanne, France
²ARCOFLUID, Talence, France

E-mail : eric.georin@cetiat.fr; general@arcofluid.fr

Introduction

The LNE-CETIAT started a modeling activity about evaporation / condensation phenomena. This present work is applied to humid air generator in order to develop a generic tool using humid air concepts. The numerical simulations have been done with the general finite volume code PHOENICS with customization in order to tackle the evaporation/condensation process.

Basically, the first step of this numerical work has been to solve the coupled conservation equations for mass, momentum and energy applied to a cylindrical geometry. In addition as the humid air may be considered like a binary mixture between dry air and water steam, a specie equation is also solved in order to describe the advection-diffusion of water steam. At last, as the main purpose deals with humidity, fundamental scalar equations of humidity are also computed. The system studied is a water pool inside a cylinder, the main part of heat and mass exchange appear at the interface level between air and water. Thus an original work has been done about the boundary conditions at the interface to account for the evaporation and/or condensation occurring at this interface in terms of mass and energy sinks and/or sources.

Geometry

Equations

Thermophysical properties

Initial conditions:
 $\vec{v}(X, t=0) = 0$ / velocity [$m \cdot s^{-1}$]
 $T(X, t=0) = T_{int}$ / temperature [$^{\circ}C$]
 $p(X, t=0) = p_{int}$ / pressure [Pa]
 $\rho(X, t=0) = \rho_{int}$ / density [$kg \cdot m^{-3}$]
 $q(X, t=0) = q_{int}(T_{int})$ / mass fraction defines as $q = \frac{m_{vapor}}{m_{air} + m_{vapor}}$

Internal domain: $\Omega = [0; R] \times [0; 2\pi] \times [0; Z]$
 with $R = 0,035 m$ and $Z = 0,07 m$
Boundary domain: $\Gamma = \Gamma_{top} \cup \Gamma_{bottom} \cup \Gamma_{interface}$
Surface normal: \vec{n}_i
Space variables: $X = \begin{pmatrix} r \\ \theta \\ z \end{pmatrix}$ with $r \in [0; R]$, $\theta \in [0; 2\pi]$, $z \in [0; Z]$

Equations

Continuity:
 $\frac{\partial \rho}{\partial t} + \nabla \cdot (\rho \vec{v}) = \dot{m}$

Momentum:
 $\rho \left(\frac{\partial \vec{v}}{\partial t} + \vec{v} \cdot \nabla \vec{v} \right) = \vec{f}_{ext} - \nabla p - \vec{\tau}$

Energy:
 $\rho c_p \left(\frac{\partial T}{\partial t} + \vec{v} \cdot \nabla T \right) = \nabla \cdot \lambda \nabla T + S_{lateral heat}$

Specie:
 $\rho \left(\frac{\partial q}{\partial t} + \vec{v} \cdot \nabla q \right) = \nabla \cdot \rho D_{diff} \nabla q$

Hypothesis

- Interface considered non-deformable.
- Temperature in liquid is homogeneous
- Gas mixture (dry air + water vapor) behaves as perfect gas

Thermophysical properties

Density:
 $\rho_{h.a.} = \frac{M_a}{R \cdot T} (p_{dry} - e + \delta \cdot e)$ [$kg \cdot m^{-3}$]
 $\rho_{h.a.} = (1,176 \cdot 10^{-6} \cdot T^{1,75}) \cdot 10^{-4}$ [$m^2 \cdot s^{-1}$]

Fickian diffusion coefficient of water steam in air:
 $D_{M} = 0,02397 + 7,590 \cdot 10^{-5} \cdot T$ [$W \cdot m^{-1} \cdot K^{-1}$]

Thermal conductivity of humid air:
 $\lambda_{h.a.} = 0,02397 + 7,590 \cdot 10^{-5} \cdot T$ [$W \cdot m^{-1} \cdot K^{-1}$]

Dynamic viscosity of humid air:
 $\mu_{h.a.} = (1,719 + 0,0429 \cdot T) \cdot 10^{-6}$ [Pa.s]

Caloric capacity of dry air:
 $c_{p,d.a.} = f(T)$ [$J \cdot kg^{-1} \cdot K^{-1}$]

Caloric capacity of water vapor:
 $c_{p,h2O vap} = f(T)$ [$J \cdot kg^{-1} \cdot K^{-1}$]

Mixing law:
 $c_{p,h.a.} = c_{p,d.a.} + q \cdot (c_{p,h2O vap} - c_{p,d.a.})$ [$J \cdot kg^{-1} \cdot K^{-1}$]

Latent heat:
 $l_v = f(T)$ [$J \cdot K^{-1}$]

Closed system

Boundary conditions:
 $\vec{v}(X \in \Gamma_{top} \cup \Gamma_{wall} \cup \Gamma_{interface}, t) = 0$
 $-\rho \frac{D_M}{1-q} \frac{\partial q}{\partial n} \Big|_{\Gamma_{interface}, t} = \dot{m}$
 $S_{lateral heat} \Big|_{\Gamma_{interface}, t} = m \cdot l_v \cdot dt$

Thermal disturbance:
 $T(\Gamma_{top} \cup \Gamma_{wall}, t < 50 s) = T_{int}$
 $T(\Gamma_{top} \cup \Gamma_{wall}, 50 s \leq t \leq 50 s) = T_{int} + A \cdot t$
 $T(\Gamma_{top} \cup \Gamma_{wall}, t > 50 s) = T_{final}$

Case 1	Case 2
$T(X, t=0) = 10^{\circ}C$	$T(X, t=0) = 50^{\circ}C$
$p(X, t=0) = 101325$	$p(X, t=0) = 101325$
$\rho(X, t=0) = 1,241 kg \cdot m^{-3}$	$\rho(X, t=0) = 1,041 kg \cdot m^{-3}$
$q(X, t=0) = 7,606 \cdot 10^{-2}$	$q(X, t=0) = 7,995 \cdot 10^{-2}$

Open system

	Case 1	Case 2	Case 3	Case 4	Case 5
T_{int}	10 $^{\circ}C$	50 $^{\circ}C$	10 $^{\circ}C$	50 $^{\circ}C$	50 $^{\circ}C$
p_{int}	101325	101325	101325	101325	101325
ρ_{int}	1,241	1,041	1,241	1,041	1,041
q_{int}	0,076	0,079	0,076	0,079	0,079
\dot{m}	0,009	0,010	0,009	0,010	0,010

	Case 1	Case 2	Case 3	Case 4	Case 5
q_{in}	0,076	0,079	0,076	0,079	0,079
q_{out}	0,000	0,000	0,000	0,000	0,000
q_{int}	0,076	0,079	0,076	0,079	0,079
q_{out}	0,000	0,000	0,000	0,000	0,000
q_{int}	0,076	0,079	0,076	0,079	0,079
q_{out}	0,000	0,000	0,000	0,000	0,000

Boundary conditions:
 $\vec{v}(X \in \Gamma_{top}, t) = 0$
 $T(X \in \Gamma_{top}, t) = T_{int}$
 $q(X \in \Gamma_{top}, t) = q_{in}$
 $\rho(X \in \Gamma_{top}, t) = \rho_{in}$

Inlet conditions:
 $q_{in}(X \in \Gamma_{top}, t) = q_{in}$
 $\rho_{in}(X \in \Gamma_{top}, t) = \rho_{in}$
 $T_{in}(X \in \Gamma_{top}, t) = T_{int}$

Outlet conditions:
 $q_{out}(X \in \Gamma_{out}, t) = q_{out}$
 $\rho_{out}(X \in \Gamma_{out}, t) = \rho_{out}$
 $T_{out}(X \in \Gamma_{out}, t) = T_{int}$

Conclusion

This work presented the modeling tool which is under development at LNE-CETIAT using the Phoenix software from CHAM Ltd (Wimbledon, UK). The model presented here is limited at the humid air part in 3D. The coupled conservation equations of momentum, mass, energy and specie are solved. Thermo physical properties varying with temperature are implemented as well as scalar quantity dedicated to humid air. An original treatment of the boundary conditions allowed to account for the latent heat exchange and the evaporation on the temperature range between 0°C and 100°C. The cases studied are divided in close and open system. Thanks to the closed system the pure diffusion model has been validated as well as specific humid air quantity. With the open systems the saturator efficiency may be computed and may give confidence in humid air generator designing.

Further this model will be developed in order to integrate the condensation phenomenon and to implement a more realistic geometry which fit more closely the real humid air generator.